Biochimica et Biophysica Acta 896 (1987) 64–76
Elsevier

BBA 73199

Depth-dependent fluorescent quenching of a tryptophan residue located at defined positions on a rigid 21-peptide helix in liposomes

Klaus-Peter Voges [a], Günther Jung [a] and William H. Sawyer [b]

[a] *Institut für Organische Chemie, Universität Tübingen, Tübingen (F.R.G.)*
and [b] *Russell Grimwade School of Biochemistry, University of Melbourne, Parkville (Australia)*

(Received 1 August 1986)

Key words: Membrane–protein interaction; Alamethicin analog; Tryptophan fluorescence; Fluorescence quenching; Circular dichroism; Doxyl stearic acid

Five lipophilic 21-peptide analogs of the potential-dependent pore-former, alamethicin, were synthesized bearing tryptophan residues at the position 1, 6, 11, 16 and 21 on a long, conformationally rigid, α-helix. The α-helical conformation was induced and stabilized using the sequential oligomers (Ala-Aib-Ala-Aib-Ala)$_n$ as analyzed by CD and NMR. The partitioning of the *N*-*t*-butoxycarbonyl 21-peptide methyl esters and the *N*-terminally deprotected α-helices was followed by fluorescence enhancement in phospholipid bilayer vesicles. Quenching experiments were performed by titrating with *n*-doxyl stearic acids bearing the nitroxide label at positions 5, 7, 10, 12 and 16. This well-defined system revealed that the N- and C-terminal tryptophan residues become situated in the hydrophilic region. Tryptophan at position 11 was found in the lipophilic core, whereas the tryptophan at positions 6 and 16 were localized at intermediate depths of the lipid membrane. Therefore, the helices span the lipid bilayer with their long axis normal to the membrane surface.

Introduction

A variety of α helical polypeptides are known to form voltage-dependent pores in lipid bilayer membranes: alamethicin [1], suzukacillin [2], trichotoxin A40 [3], and several natural and chemically modified analogs, a synthetic nonadecapeptide, melittin, and modified analogs [4]. Simple analogs of natural helical peptides such as Boc-(LAla-Aib-Ala-Aib-Ala)$_n$-OMe ($n = 1$–4) also induce voltage-dependent, ion-conducting pores, although at higher concentrations than alamethicin [5,6]. It has been concluded that a lipophilic, rigid and α-helical rod is a sufficient prerequisite for the formation of voltage-gated pores. The opening and closing of ion-conducting pores has been explained by a flip-flop within aggregates of antiparallel and parallel arranged helix dipoles in the bilayer [7]. Rigid α-helices may be used also as carriers for drugs such as hormones or for the presentation of antigens on cell surfaces [8].

These applications and the interpretation of results in bilayer experiments require a detailed knowledge of the behavior and position of the helices within the membrane. Recently the quenching processes of *n*-anthroyloxy stearic acids and *n*-doxyl stearic acids in egg-yolk phosphatidylcholine vesicles were investigated [9,10]. On this basis we were able to check the transverse disposition of helical peptides carrying a

Abbreviations: Aib (or α), α-aminoisobutyric acid; Boc, *t*-butoxycarbonyl; *n*-NS, *n*-doxyl stearic acids ($n = 5$, 7, 10, 12, 16). See also Scheme I.

Correspondence: Dr. G. Jung, Institut für Organische Chemie, Universität Tübingen, Auf der Morgenstelle 18, D-7400 Tübingen 1, F.R.G.

tryptophan fluorophore, using the set of *n*-doxyl stearic acids as a gauge within the membrane. In order to obtain suitable helices we modified the icosapeptide Boc-(L-Ala-Aib-Ala-Aib-Ala)$_4$-OMe, the pore-forming properties of which had been investigated [5,6], by incorporating a tryptophan residue at different positions. Thus a set of five henicosapeptides resulted with tryptophan at the sequence positions 1,6,11,16 and 21.

Materials and Methods

Phospholipid vesicles

Unilamellar vesicles of egg-yolk phosphatidylcholine (Lipid Products, U.K.) were prepared as described previously [11,12]. Sonication of the liposome suspension was performed with a probe-type sonicator (MSE Soniprep 150) for 4 × 30 s burst, with cooling periods between each burst. The final suspension contained 0.1 mM phospholipid in 0.1 M Tris-HCl buffer (pH 7.0).

n-Doxyl stearates

Quenching of tryptophan fluorescence was carried out using *n*-doxyl stearates (*n*-NS, $n = 5,7,10,12$) purchased from Molecular Probes (U.S.A.).

Peptide syntheses

The peptides were synthesized by fragment condensation as outlined in Fig. 1. Boc-LAla-Aib-Ala-Aib-Ala-OH [13], Boc-LAla-Aib-Ala-Aib-Ala)$_2$-OH and H-(LAla-Aib-Ala-Aib-Ala)$_n$-OMe HCl ($n = 1$–4) [14] were the key products for the synthesis of the tryptophan helices. The syntheses [14], spectroscopic studies [14,15] and dipole moments [16] of the helices Boc-(Ala-Aib-Ala-Aib-Ala)$_n$-OMe ($n = 1$–4) were published elsewhere. The identity and purity of the tryptophan-containing helices was checked by TLC (detection with ninhydrin and chlorine/4,4′-methylenebis(*N*,*N*′-dimethylaniline) TDM reagent), amino-acid analysis (addition of thioglycolic acid to 6 M HCl,

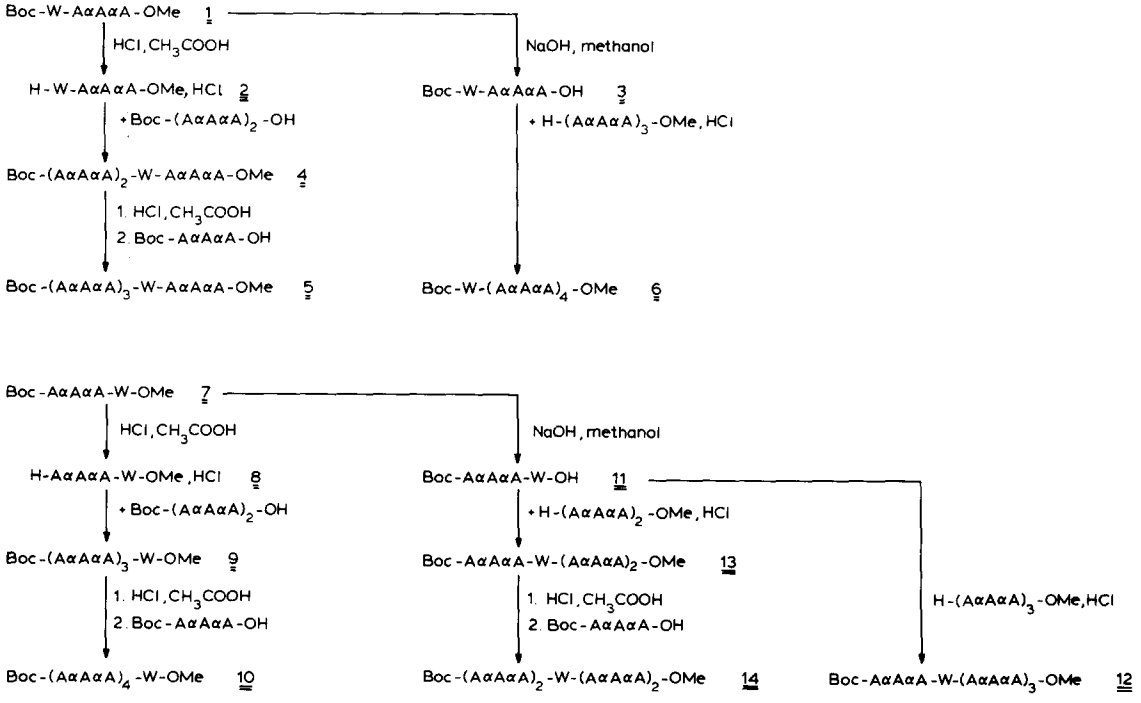

Fig. 1. Scheme of fragment condensations used for the synthesis of five tryptophan-containing α-helical 21-peptides (A, alanine: α = α-aminoisobutyric acid; Boc = *tert*-butoxycarbonyl; W, tryptophan).

110°C, 18 h), and ^{1}H-NMR. R_F values were determined on silica-gel plates (Merck, No. 5729) with chloroform/methanol/acetic acid/ (65 : 25 : 3 : 4, v/v).

Boc-Trp-Ala-Aib-Ala-Aib-Ala-OMe (1)

At −10°C, a 1 M solution of *N,N'*-dicyclohexylcarbodiimide in dichloromethane (1.43 ml, 1.43 mmol) is added to Boc-Trp-OH (402 mg, 1.32 mmol) and 1-hydroxybenzotriazole (180 mg, 1.32 mmol) in dimethylformamide (1 ml). After 10 min at −10°C, *N,N'*-dicyclohexylurea precipitates and H-Ala-Aib-Ala-Aib-Ala-OMe · HCl [13] (500 mg, 1.1 mmol) and *N*-methylmorpholine (0.121 ml, 1.1 mmol) in dimethylformamide (3 ml) are added. After 1 h at −10°C, 4 h at 0°C, and 18 h at room temperature acetic acid (50 µl) is added and the urea is removed by centrifugation. The supernatant is concentrated in vacuo, and the dry residue is dissolved in ethyl acetate/1-butanol (1 : 1, v/v) and washed thrice with 5% sodium hydrogen carbonate, thrice with 5% potassium hydrogen sulfate and five time with water. After drying over sodium sulfate Boc-Trp-Ala-Aib-Ala-Aib-Ala-OMe (**1**) is precipitated by addition of light petroleum (b.p. 30–50°C), and chromatographed on Sephadex LH-20 (column 60 × 2.7 cm). Yield: 680 mg (88%); $R_F = 0.81$.

H-Trp-Ala-Aib-Ala-Aib-Ala-Aib-Ala-OMe –HCl (2)

Hexapeptide **1** (200 mg, 0.285 mmol) is deprotected with 1.2 M HCl/acetic acid (1.54 ml, 1.85 mmol) at 5°C. After 10 min the solution is concentrated in vacuo, the dry residue is dissolved in methanol and evaporated again. After freeze-drying from *t*-butanol/water (3 : 1) the ester is stored over potassium hydroxide in vacuo. Yield: 173 mg (95%); $R_F = 0.86$.

N-Boc-Trp-Ala-Aib-Ala-Aib-Ala-OH (3)

Hexapeptide **1** (200 mg, 0.285 mmol) is saponified in methanol (7.5 ml) and 0.5 M NaOH (1.73 ml, 0.86 mmol). After 2 h at room temperature the solution is neutralized at 0°C, and methanol is removed on a rotary evaporator. After acidification to pH 2 and extraction with ethyl acetate (five times) the combined extracts are washed twice with water, dried over sodium sulfate and evaporated in vacuo. The hexapeptide acid **3** is chromatographed on Sephadex LH-20 and freeze-dried from *t*-butanol/water (3 : 1). Yield: 154 mg (80%); $R_F = 0.42$.

Boc-(Ala-Aib-Ala-Aib-Ala)$_2$-Trp-Ala-Aib-Ala-Aib-Ala-OMe (4)

Boc-(Ala-Aib-Ala-Aib-Ala)$_2$-OH [14] (150 mg, 0.17 mmol) is activated at 0°C with 1-hydroxybenzotriazole (23 mg, 0.17 mmol) in dimethylformamide (1.5 ml) by addition of *N,N'*-dicyclohexylcarbodiimide (38.5 mg, 0.19 mmol). After precipitation of urea the mixture is warmed up to room temperature, and after 15 min the hexapeptide ester hydrochloride (**2**) (130 mg, 0.2 mmol) and *N*-methylmorpholine (22 µl, 0.2 mmol) in dimethylformamide (1 ml) are added. After 18 h, acetic acid (50 µl) is added, the urea is removed by centrifugation, and the supernatant is concentrated in vacuo. The residue is dissolved in dichloromethane and purified as described for **1**. Yield: 240 mg (95%); $R_F = 0.85$.

Boc-(Ala-Aib-Ala-Aib-Ala)$_3$-Trp-Ala-Aib-Ala-Aib-Ala-OMe (5)

Hexapeptide **4** (240 mg, 0.165 mmol) is dissolved in 1.2 M HCl/acetic acid (2 ml) and concentrated in vacuo after 10 min. After drying in a desiccator over potassium hydroxide, the peptide ester is dissolved in dimethylformamide (2 ml) and neutralized with *N*-methylmorpholine (18 µl, 0.165 mmol). Boc-Ala-Aib-Ala-Aib-Ala-OH [13,14] (166 mg, 0.33 mmol) is activated at 0°C with 1-hydroxybenzotriazole (45 mg, 0.33 mmol) in dimethylformamide (1.5 ml) and *N,N'*-dicyclohexylcarbodiimide (39 mg, 0.19 mmol). After precipitation of urea the activated pentapeptide acid is added to the solution of the hexadecapeptide ester. After 18 h, acetic acid (50 µl) is added and the solvent is evaporated in vacuo. The henicosapeptide, **5**, is purified on Sephadex LH-20 in dichloromethane/methanol (11 : 1, v/v). Further purification is achieved on a silica-gel column followed again by Sephadex LH-20 chromatography. Yield: 89 mg (30%); $R_F = 0.70$; m.p. 205°C (dec.).

Boc-Trp-(Ala-Aib-Ala-Aib-Ala)$_4$-OMe (6)

This 21-peptide can be prepared via two differ-

ent routes. Boc-Trp-OH (28.5 mg, 95 μmol) is activated at 0°C with 1-hydroxybenzotriazole (13 mg, 94 mmol) in dimethylformamide (0.5 ml) and *N,N'*-dicyclohexylcarbodiimide (21 mg, 19 μmol). After precipitation of urea, the mixture is pipetted into a solution of H-(Ala-Aib-Ala-Aib-Ala)$_4$-OMe · HCl (30 mg, 19 μmol) and *N*-methylmorpholine (19 μl, 19 μmol) in dimethylformamide/dichloromethane (1 : 1, v/v; 200 μl). After 4 h the icosapeptide ester has disappeared (TLC), and the isolation of **6** is performed as described for **5**. Yield: 10 mg (29%); $R_F = 0.70$.

Boc-Trp-Ala-Aib-Ala-Aib-Ala-OH (101 mg, 148 μmol) is activated at 0°C with 1-hydroxybenzotriazole in dimethylformamide (1.5 ml) and *N,N'*-dicyclohexylcarbodiimide (37 mg, 1.80 μmol). A solution of H-(Ala-Aib-Ala-Aib-Ala)$_3$-OMe (150 mg, 123 μmol) and *N*-methylmorpholine (14 μl, 123 μmol) in dimethylformamide (1.5 ml) is added. After 10 h at room temperature the polypeptide **6** is isolated as described for **5**. Yield: 70 mg (31%); $R_F = 0.70$.

Boc-Ala-Aib-Ala-Aib-Ala-Trp-OMe (7)

To Boc-Ala-Aib-Ala-Aib-Ala-OH (575 mg, 1.15 mmol) and 1-hydroxybenzotriazole (156 mg, 1.15 mmol) in dimethylformamide (5 ml) is added a 1 M solution of *N,N'*-dicyclohexylcarbodiimide in dichloromethane (1.26 ml, 1.26 mmol) at 0°C. After 30 min (precipitation of urea) H-Trp-OMe · HCl (350 mg, 1.38 mmol) and *N*-methylmorpholine (152 μl, 1.38 mmol) in dimethylformamide is added. After 24 h at room temperature the isolation follows the procedure for **1**. The hexapeptide **7** is purified by gel chromatography on Sephadex LH-20. Yield: 565 mg (70%); $R_F = 0.90$.

H-Ala-Aib-Ala-Aib-Ala-Trp-OMe · HCl (8)

Hexapeptide **7** (400 mg, 570 μmol) is deprotected in 1.2 M HCl/acetic acid (3 ml, 3.7 mmol) at 0°C. After 10 min the solution is concentrated in vacuo. The dry residue is dissolved in methanol and evaporated again several times, and lyophilized from *t*-butanol/water (3 : 1, v/v). Yield: 291 mg (80%); $R_F = 0.45$.

Boc-(Ala-Aib-Ala-Aib-Ala)$_3$-Trp-OMe (9)

Boc-(Ala-Aib-Ala-Aib-Ala)$_2$-OH (176 mg, 197 μmol) is activated at 0°C with hydroxybenzotriazole (27 mg, 197 μmol) in dimethylformamide (1.5 ml) and a 1 M solution of *N,N'*-dicyclohexylcarbodiimide in dichloromethane (215 μl, 215 μmol). After precipitation of urea (15 min) a solution of hexapeptide ester **8** (105 mg, 164 μmol) and *N*-methylmorpholine (17 μl, 164 μmol) in dimethylformamide (1 ml) is added. After 15 h the hexadecapeptide is isolated according to the procedure described for **5**. Chromatography on Sephadex LH-20, silica gel and again Sephadex LH-20 in methanol yield peptide **9**. Yield: 200 mg (83%); $R_F = 0.85$.

Boc-(Ala-Aib-Ala-Aib-Ala)$_4$-Trp-OMe (10)

Hexapeptide ester **9** (300 mg, 204 μmol) is deprotected with 1.2 M HCl/acetic acid at 5°C. After 10 min the solution is evaporated and the residue is dried over KOH in vacuo for 12 h. The ester and *N*-methylmorpholine (23 μl, 399 μmol) are dissolved in dimethylformamide (2 ml) and a solution of Boc-Ala-Aib-Ala-Aib-Ala-OH (200 mg, 399 μmol), preactivated with 1-hydroxybenzotriazole (54 mg, 399 μmol) and 1 M *N,N'*-dicyclohexylcarbodiimide/dichloromethane (440 μl, 440 μmol) in dimethylformamide/dichloromethane (1 : 1, 2 ml) is added. Acetic acid (50 μl) is added after 18 h and the henicosapeptide **10** is isolated as described for **5**. Yield: 100 mg (27%); $R_F = 0.85$; m.p. 170°C (dec.).]

Boc-Ala-Aib-Ala-Aib-Ala-Trp-OH (11)

Hexapeptide ester **7** (200 mg, 0.28 mmol) was saponified in methanol (7.5 ml) with 0.5 M NaOH (1.73 ml, 0.86 mmol). After 2 h the hexapeptide acid **11** was isolated as described for **3** and chromatographed on silica-gel and Sephadex LH-20 in methanol. Yield 170 mg (88%); $R_F = 0.42$; m.p. 195°C (dec.).

Boc-Ala-Aib-Ala-Aib-Ala-Trp-(Ala-Aib-Ala-Aib-Ala)-OMe (12)

Hexapeptide acid **11** (113 mg, 164 μmol) in dichloromethane (1.5 ml) is activated with 1-hydroxybenzotriazole (22 mg, 164 μmol) and *N,N'*-dicyclohexylcarbodiimide (37.3 mg, 180.5 μmol) at 0°C. After the activation becomes evident (precipitation of urea) H-(Ala-Aib-Ala-Aib-Ala)$_3$-OMe [14] (100 mg, 82 μmol) and *N*-methylmorpholine (9 μl, 82 μmol) in dimethylformamide (1 ml) are

added. After 4 h acetic acid (40 μl) is added, the solvent is removed and the residue is dissolved in dichloromethane. After filtering off the insoluble urea, the peptide **12** is chromatographed on Sephadex LH-20, silical-gel and again on Sephadex LH-20 in methanol/dichloromethane (1 : 1, v/v). Yield 150 mg (49%); $R_F = 0.78$; m.p. 172°C (dec.).

Boc-Ala-Aib-Ala-Aib-Ala-Trp-(Ala-Aib-Ala-Aib-Ala)$_2$-OMe (13)

Hexapeptide acid **11** (200 mg, 0.29 mmol) is activated with 1-hydroxybenzotriazole (39 mg, 0.29 mmol) and *N,N'*-dicyclohexylcarbodiimide (70 mg, 0.34 mmol) in dimethylformamide (2 ml) at 0°C. After 10 min H-(Ala-Aib-Ala-Aib-Ala)$_2$-OMe · HCl (202 mg, 0.24 mmol) in dimethylformamide (1.5 ml) are added. After 18 h and addition of acetic acid (50 μl) the filtrate of the reaction mixture is evaporated and the residue is taken up in chloroform and washed with 5% potassium hydrogen sulfate and water. Final purification of **13** is achieved by gel chromatography on Sephadex LH-20. Yield: 300 mg (84%); $R_F = 0.72$; m.p. 170°C.

Boc-(Ala-Aib-Ala-Aib-Ala)$_2$-Trp-(Ala-Aib-Ala-Aib-Ala)$_2$-OMe (14)

Hexapeptide **13** (300 mg, 204 μmol) is deprotected in 1.2 M HCl/acetic acid (2 ml, 204 μmol) at 0°C. After 10 min the solvent is removed and the resulting peptide ester hydrochloride is chromatographed on Sephadex LH-20 in methanol in order to remove decomposition products. The main fraction (200 mg, 143 μmol, yield 70%) and *N*-methylmorpholine (16 μl, 143 μmol) are dissolved in dimethylformamide (1.5 ml). Boc-Ala-Aib-Ala-Aib-Ala-OH [13] (143 mg, 285 μmol) is activated with 1-hydroxybenzotriazole (39 mg, 285 μmol) and *N,N'*-dicyclohexylcarbodiimide (65 mg, 314 μmol) in dichloromethane and, after 10 min, is added to the hexadecapeptide ester. After 5 h acetic acid (50 μl) is added, the solution is evaporated and the residue chromatographed on Sephadex LH-20, silica-gel, and again on Sephadex LH-20 in dichloromethane/methanol (1 : 1, v/v). Yield: 103 mg (49%); $R_F = 0.70$; m.p. 173°C (dec.).

21-Peptide methyl esters with free N-terminus

After treatment of henicosapeptides **5, 6, 10, 12** and **14** with HCl/acetic acid for 10 min at 4°C, a second set of henicosapeptides is obtained possessing free, positively charged N-terminus. After lyophilisation from *t*-butanol these peptides are checked by TLC, CD, ultraviolet and fluorescence spectroscopy.

Analyses of tryptophanyl peptides

The *N*-Boc-protected hexapeptides **1, 3, 7** and **8** were characterized by ^{1}H- and ^{13}C-NMR spectra. After acidolytic removal of the *t*-butoxycarbonyl group the hexapeptide ester hydrochlorides **2** and **8** were analyzed by ^{1}H-NMR and found to contain the intact indolyl ring. On the amino-acid analyzer, peak separation of Ala/Aib could not be achieved quantitatively (ratio of color factors Ala/Aib = 7 : 1) for the five henicosapeptides. Threfore the Ala/Aib and the Trp peaks (addition of thioglycolic acid for hydrolysis) were taken for the determination of recovery factors. Only Boc-Trp-(Ala-Aib-Ala-Aib-Ala)$_4$-OMe (**6**) contained larger amounts of silica gel (recovery factor 0.26), whereas the other four 21-peptides showed excellent recovery factors: 1.00(**12**), 0.98 (**14**), 0.95(**5**) and 0.95(**10**). Gas chromatography of the *N*-pentafluoropropionylamino acid *n*-propyl esters of the hydrolysate (prepared in the presence of 2-propanethiol) on a Chirasil-Val capillary column gave satisifying results.

The analyses of all peptides which do not contain tryptophan are reported elsewhere [13–15].

Spectroscopy

Ultraviolet spectra of the polypeptides were measured in ethanol at concentrations from $c = 1 \cdot 10^{-7}$ to $c = 1 \cdot 10^{-8}$ mol/l on a Cary ultraviolet spectrometer (path-length $d = 1$ cm; slit-width 1 nm; temperature 22°C). Circular dichroism spectra were measured on a CD 195 spectrometer (Roussel-Jouan) in methanol ($c = 1 \cdot 10^{-3}$ mol/l; temperature 20°C). The intensity of the Cotton effects is given in mean residue ellipticities $[\theta]_m$. Epiandosterone in dioxan with $[\theta] = 10.925$ deg · cm^2 · dmol^{-1} at 304 nm was used for calibration of the spectrometer. Fluorescence spectra of tryptophan-containing peptides were recorded with a

Hitachi-Perkin Elmer MPF3 spectrofluorimeter using an excitation wavelength of 290 nm. Peptide solutions ($c = 4 \cdot 10^{-6}$ mol/l) were prepared in the following solvents: (a) 0.1 M Tris-HCl (pH 7.0); (b) ethanol; (c) 0.1 mM egg phosphatidylcholine vesicles in 0.1 M Tris-HCl buffer (pH 7.0).

Quenching experiments

Stock solutions (1 mM) of the *n*-doxyl stearic acids (*n*-NS) were prepared in methanol and their relative concentrations measured by ESR. Aliquots (6×5 µl) were added to 2.5 ml of vesicle suspension (0.1 mM phospholipid containing 4 µM peptide) in a cuvette, and the fluorescence intensity was determined at 340 nm. The use of *n*-NS probes to determine the transverse position of fluorophore bilayers requires a knowledge of the partition coefficients of the quenchers. These were determined according to methods published elsewhere [9,10].

Analysis of peptide partitioning

The partitioning [17] of the polypeptides into the bilayer phase was determined by analysis of the enhancement of tryptophan fluorescence that occurs during uptake. At a given concentration of peptide and membrane, the observed fluorescence is determined by the fluorescence of the peptide in the membrane (M) and aqueous (A) phases.

$$F_{obs} = F_M + F_A \quad (1)$$

$$= F_M \cdot f + F_A(1 - f) \quad (2)$$

where f is the fraction of total peptide which is in the lipid phase.

$$f = \frac{F_{obs} - F_A}{F_M - F_A} \quad (3)$$

The concentration of the peptide in the membrane ($[P]_M$) is given by:

$$[P]_M = [P]_T \cdot f = \langle P \rangle \cdot [ves] \quad (4)$$

where $[P]_T$ is the total concentration of peptide, $\langle P \rangle$ is the number of peptide molecules per vesicle, and [ves] is the concentration of vesicles. The total concentration of peptide is the sum of the concentration in each phase:

$$[P]_T = [P]_M + [P]_A \quad (5)$$

$$= \langle P \rangle \cdot [ves] + [P]_A \quad (6)$$

Thus, uptake experiments at a range of vesicle concentrations provide data for a plot of Eqn. 6, values of $\langle P \rangle$ and $[P]_A$ being determined from the slope and intercept, respectively. The concentration of peptide in the lipid phase, expressed with respect to the volume of the lipid phase becomes:

$$[P]_L = \langle P \rangle = K_p \cdot [P]_A \quad (7)$$

where K_p is the partition coefficient and V_L is the volume of 1 mol of vesicles. K_p can therefore be determined from a plot of $\langle P \rangle$ versus $[P]_A$. Where the uptake is determined by binding to predetermined sites on or in the membrane, as well as by partition, the ordinate intercept of this plot can provide a measure of the number of binding sites [9].

Results and Discussion

By conventional peptide fragment condensations five α-helices were synthesized (compare Fig. 1) each containing one tryptophan residue. According to the sequence position of the tryptophan residue the *t*-butoxycarbonyl-protected henicosapeptides (21-peptides) and the corresponding *N*-deprotected peptides used in this investigation were abbreviated as shown in Scheme I.

Boc-W-(AαAαA)$_4$-OMe **6**	B-21$_1$-OMe
+ H$_2$-W-(AαAαA)$_4$-OMe	H-21$_1$-OMe
Boc-AαAαA-W-(AαAαA)$_3$-OMe **12**	B-21$_6$-OMe
+ H$_2$-AαAαA-W-(AαAαA)$_3$-OMe	H-21$_6$-OMe
Boc-(AαAαA)$_2$-W-(AαAαA)$_2$-OMe **14**	B-21$_{11}$-OMe
+ H$_2$-(AαAαA)$_2$-W-(AαAαA)$_2$-OMe	H-21$_{11}$-OMe
Boc-(AαAαA)$_3$-W-AαAαA-OMe **5**	B-21$_{16}$-OMe
+ H$_2$-(AαAαA)$_3$-W-AαAαA-OMe	H-21$_{16}$-OMe
Boc-(AαAαA)$_4$-W-OMe **10**	B-21$_{21}$-OMe
+ H$_2$-(AαAαA)$_4$-W-OMe	H-21$_{21}$-OMe

Scheme I. Peptide abbreviations.

The conformationally stable α-helical henicosapeptides with tryptophan in defined positions were embedded in liposomes and examined as follows:

(a) Upon excitation at 290 nm the Stokes' shift of the emission band was recorded for the henicosapeptides in solvents of different polarity.

(b) The partition coefficients in the polypeptides were determined from the enhancement of tryptophan fluorescence according to Eqns. 6 and 7.

(c) The liposomes were titrated with *n*-doxyl stearic acids ($n = 5, 7, 10, 12, 16$) to determine the transverse position of tryptophan residues in the bilayer.

Using this experimental approach we tried to prove that each helix buries its fluorophore at a defined depth – the depth which is predicted by perpendicular insertion of the helices into the membrane. If the fluorescent oligopeptides span the bilayer in a helical form, they could be classified into three arbitrary groups:

(1) B/H-21_1-OMe and B/H-21_{21}-OMe would have terminal fluorophores near the membrane surface.

(2) B/H-21_{11}-OMe and B/H-21_{16}-OMe would have fluorophores located within the lipophilic center of the membrane.

(3) B/H-21_6-OMe cannot be classified in an a priori way.

The above classification does not exclude the possibility that the polypeptide structures are tilted at some angle to the membrane normal.

Absorption spectra

The indolyl chromophore of the tryptophan residue showed the same wavelengths of absorption bands at 274, 282 and 290 nm for all α-helical 21-peptides (Fig. 2). The intensity ratios of these bands were about the same within the series of B-21_x-OMe, and it was assumed that the molar extinctions were independent of the position of the tryptophan residue along the α-helix. Therefore ultraviolet absorption was taken as a measure for the relative concentration within the series of B-21_x-OMe and H-21_x-OMe peptides. Not only were almost coincident ultraviolet spectra found within these two series, but the maxima of the spectra were also very similar to those of *N*-stearoyl-L-tryptophan-*n*-hexyl ester and 3-methylindole.

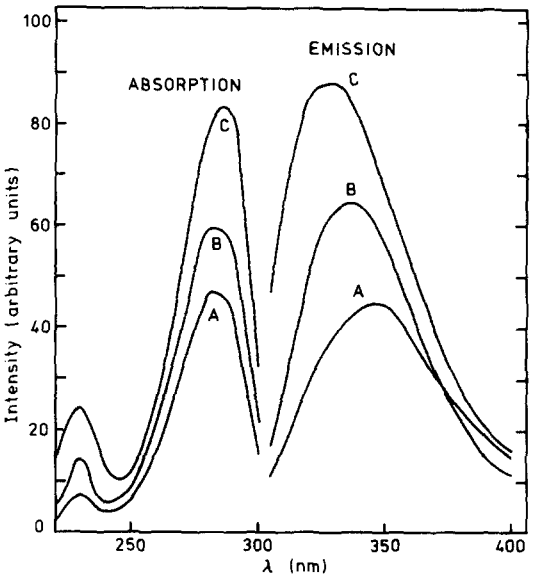

Fig. 2. Solvent dependence of the absorption and emission spectra of 21-peptide Boc-(AαAαA)$_3$-W-AαAαA-OMe (B-21_{16}-OMe, **5**) in 0.1 M Tris-HCl (pH 7.0) (A), ethanol (B) and 0.1 mM phosphatidylcholine (C).

Circular dichroism

Obviously the α-helix content is sensitive to the position of tryptophan in the polypeptide chain, which is documented by the different CD spectra of the 21-peptides (Fig. 3). Although aminoisobutyrate peptides may not be appropriate examples in this context, it should be emphasized that N-terminal tryptophan on helices has a higher α-propensity ($H_\alpha = 1.45$) than in other α-helical positions ($H_\alpha = 1.15$) [18].

Henicosapeptides of B-21_{11}-OMe and B-21_{16}-OMe have identical ultraviolet absorption, yet have different circular dichroic spectra. In methanol, higher ellipticities were observed for B-21_1-OMe, B-21_6-OMe and B-21_{21}-OMe; these peptides have ellipticities as found for alamethicin [1] and Boc-(Ala-Aib-Ala-Aib-Ala)$_3$-OMe. We found earlier that the prolongation of the latter pentadecapeptide to the icosapeptide Boc(Ala-Aib-Ala-Aib-Ala)$_4$-OMe reduces the α-helix content from 80% to 40% [14]. In the present case of the henicosapeptides B-21_1-OMe and B-21_6-OMe, the strong helix-former tryptophan restores the α-helix to 80%. It is not clear, however, why tryptophan in the C-terminal position in B-21_{21}-OMe also leads

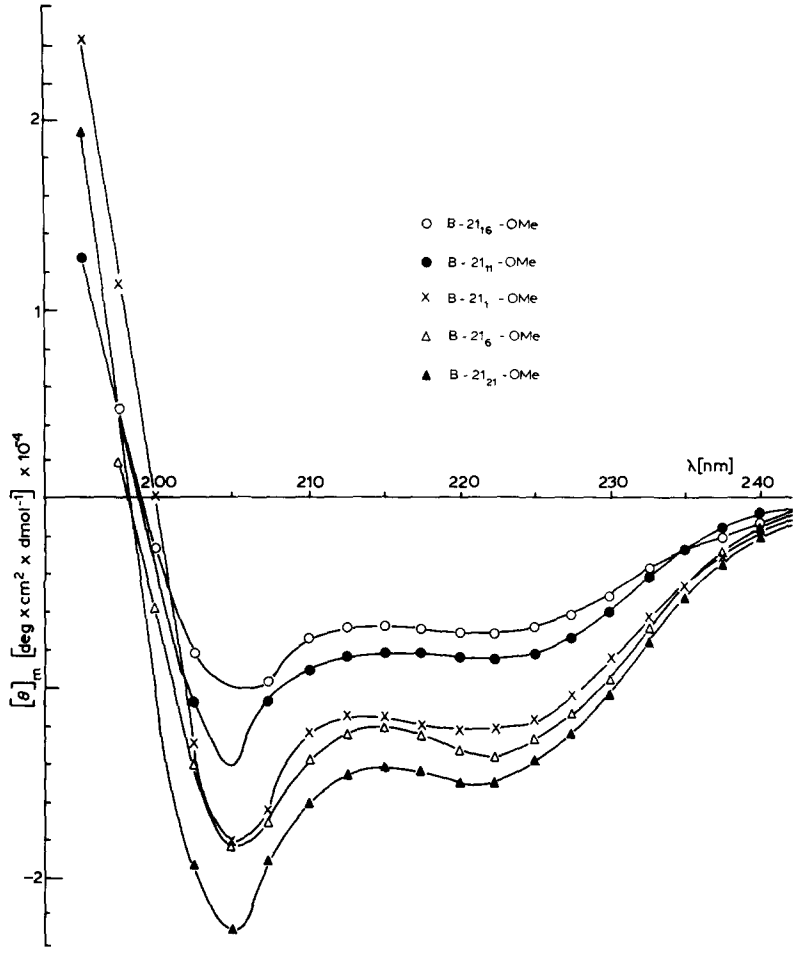

Fig. 3. Circular dichroism spectra of the five tryptophan containing α-helical 21-peptides (1 mM; ethanol, 20°C).

to high ellipticities. According to the CD measurements, the tryptophan residue in the middle of the molecule destabilizes the still-dominating α-conformation in B-21$_{11}$-OMe and B-21$_{16}$-OMe.

The CD spectra of the series are homogeneous with respect to the wavelengths of the Cotton effects and their intensity ratios (Table I). The maxima of π,π^* transitions are shifted by 2 nm to 205 nm with respect to the non-tryptophan-containing icosapeptide, Boc-(Ala-Aib-Ala-Aib-Ala)$_4$-OMe.

TABLE I

CIRCULAR DICHROISM DATA OF THE TRYPTOPHAN-HELICES B-21$_x$-OMe (METHANOL, 1 mM, 20°C)

x	1	6	11	16	21
$[\theta]_m^{205}$	−18100	−18320	−14070	−10250	−22670
$[\theta]_m^{222}$	−12200	−13590	−8500	−7190	−15000
$R = [\theta]_m^{222}/[\theta]_m^{205}$	0.67	0.74	0.60	0.70	0.66
% α-Helix	80	81	62	45	100
Residues in α-Helix	17	17	13	9-10	21

TABLE II

SOLVENT DEPENDENCE OF THE TRYPTOPHAN FLUORESCENCE MAXIMUM (nm) OF THE 21-PEPTIDE HELICES

In parentheses are given shifts ($\Delta\lambda$) of the fluorescence maximum referred to buffer solution ($\Delta\lambda = 0$).

	Tris-HCl	Ethanol	Phosphatidylcholine bilayers
Boc-21_1-OMe	346	338 (−8)	337 (−9)
H-21_1-OMe	352	342 (−10)	348 (−4)
Boc-21_6-OMe	320	330 (+10)	320 (0)
H-21_6-OMe	349	335 (−14)	322 (−27)
Boc-21_{11}-OMe	346	339 (−7)	324 (−22)
H-21_{11}-OMe	352	339 (−13)	338 (−14)
Boc-21_{16}-OMe	345	340 (−5)	330 (−15)
H-21_{16}-OMe	350	339 (−11)	332 (−18)
Boc-21_{21}-OMe	–	–	–
H-21_{21}-OMe	350	350 (0)	345 (−5)

Fluorescence spectra

The fluorescence spectra of the helical polypeptide esters **5, 6, 10, 12, 14** (Fig. 1) and their N-deprotected esters were recorded in three solvent systems:

(A) aqueous buffer (0.1 M Tris-HCl (pH 7.0));

(B) ethanol;

(C) bilayer vesicles.

Generally, a blue shift of fluorescence band is observed on changing the solvents from A to C (Fig. 2), whereas the ultraviolet band does not shift.

Due to the positively charged N-terminus, the series H-21_x-OMe is expected to form a larger solvent cage than the uncharged series B-21_x-OMe. Thus, according to the Lippert equation, the compounds H-21_x-OMe exhibit a Stokes' shift which is about 5 nm larger than for the compounds B-21_x-OMe (Table II). Both compounds, B-21_1-OMe and H-21_1-OMe, locate the fluorophore near the hydrophilic surface of the membrane, where the polarity of the environment is similar to the buffer solution, resulting in a minimal Stokes' shift (Fig. 4).

Similarly, a blue shift of only 5 nm is observed for H-21_{21}-OMe on changing the medium from buffer to ethanol to bilayer vesicles. We would expect the charged N-terminus to be about 30 Å from the fluorophore in this helical compound.

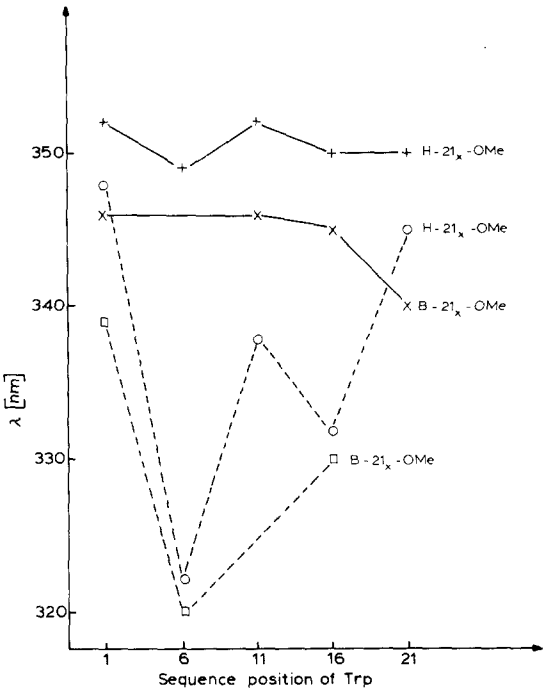

Fig. 4. Dependence of the fluorescence emission maximum on the position of the tryptophan residue in N-Boc and protonated 21-peptide helices in 0.1 M Tris-HCl (———) and in liposomes (- - - -).

Therefore, the induced small blue shift at the C-terminal tryptophan must be attributed to charge effects of N-termini of neighboring helices in antiparallel position. The fact that both N- and C-terminal fluorophores are in a polar environment leads to the conclusion that the H-21_{21}-OMe helices are inserted perpendicular to the membrane surface and span the membrane.

The behavior of B-21_6-OMe cannot be explained satisfactorily. This compound seems to agregate strongly in aqueous solution thus producing a lipophilic environment for the fluorophore. Except for B-21_{16}-OMe and H-21_{16}-OMe, the charged and uncharged species behave similarly. Obviously the positive charge at the N-terminus of the 21-peptide helices does not influence the orientation of the helix or depth of the fluorophore. This is consistent with the results of bilayer experiments, in which the N-terminally charged helices induce voltage-dependent, ion-conducting pores, but with different pore-state characteristics [5,6].

TABLE III

PARTITION COEFFICIENTS (K_p) OF THE TRYPTOPHAN α-HELICES IN EGG PHOSPHATIDYLCHOLINE BILAYERS

Peptide	K_p[cm^{-3}·mol^{-1}] ($\times 10^4$)	r [a]
B-21$_1$-OMe	1.390 ±0.42	0.89
B-21$_6$-OMe	0.632 ±0.09	0.97
B-21$_{11}$-OMe	0.461 ±0.15	0.87
B-21$_{16}$-OMe	4.570 ±0.11	0.99
Indole	3.340 ±1.0	0.95
Trp-Sta	5.700 ±0.6	-
H-21$_1$-OMe	1.560 ±0.47	0.86
H-21$_6$-OMe	1.540 ±0.23	0.99
H-21$_{11}$-OMe	3.690 ±0.50	0.97
H-21$_{16}$-OMe	3.490 ±0.52	0.97
H-21$_{21}$-OMe	80.30 ±27.6	0.83

[a] Correlation coefficient for plot of Eqn. 7 ($[P]_L$ vs. $[P]_A$).

Two conclusions may be drawn from the fluorescence spectra:
(1) B-21$_1$-OMe and H-21$_{21}$-OMe locate their terminal tryptophan fluorophores near the hydrophilic membrane surface.
(2) Helices with tryptophan in positions 6, 11 and 16 locate their fluorophores in the lipophilic, inner part of the membrane.

Fluorescence enhancement

The mechanism of association of the helical polypeptide with the lipid bilayer can be inferred from data plotted according to Eqn. 6. When partition is the only type of association process, such plots are linear and pass through the origin. When the association involves both partition and binding processes the plots are nonlinear [9]. In the present study, these plots were linear and intercepted the ordinate axis close to the origin, indicating that partition was the dominant mode of association. The K_p values for the polypeptides are summarized in Table III and confirm their high lipophilicity. These values are comparable to those determined for doxyl stearates in bilayer systems [12]. Since the overall lipophilicity of the butoxycarbonyl-protected polypeptides is the same, the observed difference in K_p must be attributed to the influence of sequence and conformation. The same is true of differences within the deprotected series of polypeptides.

Quenching of fluorescence

Table IV summarizes the expected transverse positions of the doxyl groups and tryptophan residues in the lipid bilayer for the *n*-NS and H-21$_x$-OMe molecules, respectively. After incorporation of the polypeptide into the bilayer, the highest quenching efficiency should be observed for the *n*-doxyl stearate which places its doxyl moiety closest to the tryptophan fluorophore. Quenching data are normally presented as a Stern-Volmer plot of the quenching efficiency, QE ($= I_0/I - 1$) versus total quencher concentration, $[Q]_T$; I and I_0 being the fluorescence intensities in the presence and absence of quencher, respectively. In the two-phase system dealt with here the appropriate value of [Q] is that pertaining to the lipid phase rather than to the total volume. Indeed, the use of $[Q]_T$ can lead to serious errors [9,10]. Thus, the abscissa in Figs. 5 and 6 are scaled in terms of the average number of quencher molecules per vesicle rather than $[Q]_T$.

TABLE IV

DEPTHS OF THE DOXYL LABELS AND TRYPTOPHAN RESIDUES IN A LIPID BILAYER MEMBRANE

	x =	1	6	11	16	21
H-21$_x$-OMe	d_{theor} =	1.5	9	16.5	24	31.5
	$d_{obs.}$ =	1–5	6–9	15	25	38–33
n-NS [a]	n =	5	7	10	12	16
	d =	6.25	8.75	12.5	15	20
	d' =	30.75	28.25	25.5	22	17

[a] For *n*-NS, two values for the depth of a quencher (d and d') are given, because the carboxy groups are anchored on both polar sides of the bilayer membrane (thickness: 37 Å). The theoretical depths of a fluorophore was calculated assuming an ideal α-helix spanning the membrane, using the relation $d_{theor.} = 1.5 \times n$ Å (n, sequence position of tryptophan residues). $d_{obs.}$ are the values taken from the modified Stern-Volmer plots for the observed maximal quenching efficiency.

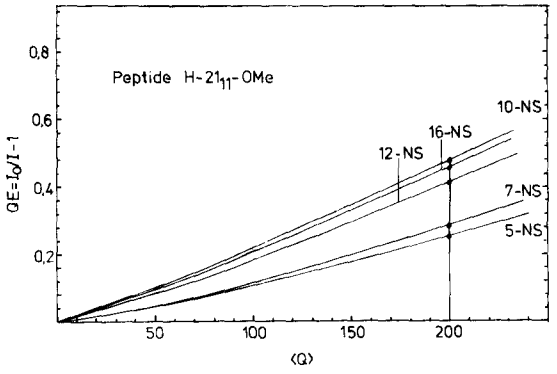

Fig. 5. Stern-Volmer plot for the quenching of the tryptophan fluorophore in H-21$_{11}$-OMe by the doxyl stearic acids *n*-NS ($n = 5, 7, 10, 12, 16$). The quenching efficiency (QE) at $\langle Q \rangle = 200$ normalized with respect to QE(5-NS) gives data for the secondary plots shown in Fig. 7.

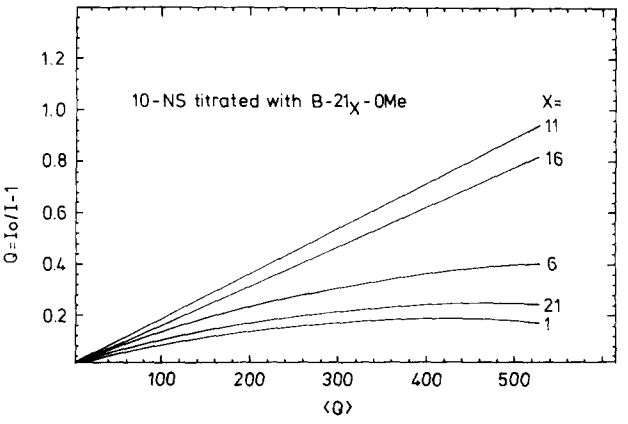

Fig. 6. Stern-Volmer plots of titration of *n*-doxyl stearic acids with the five butoxycarbonyl-protected helices B-21$_x$-OMe ($x = 1, 6, 11, 16, 21$).

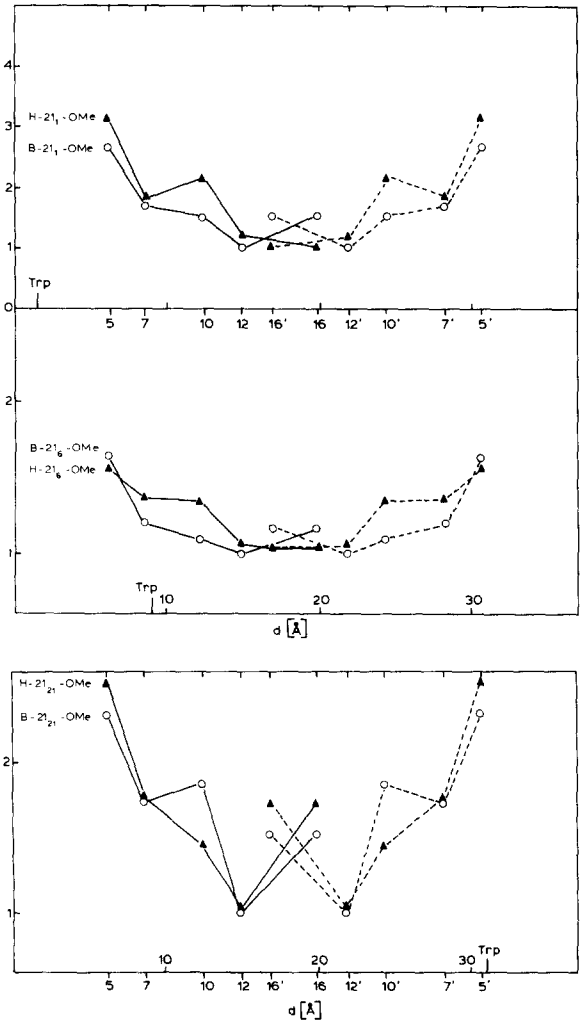

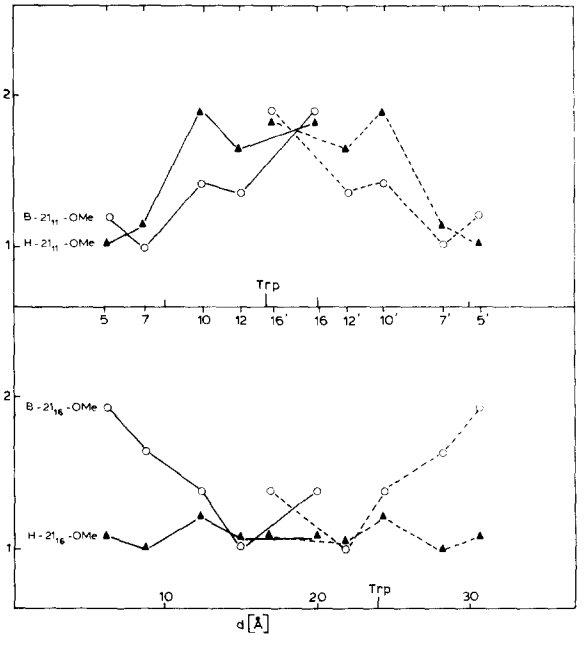

Fig. 7. Secondary plots of Stern-Volmer quenching data showing the relative quenching efficiency as a function of the transverse position of the quenching (doxyl) group in the membrane. The arrows indicate the expected transverse positions of the tryptophan residue in the butoxycarbonyl-protected (⊙) and protonated (▲) 21-peptide methylesters.

A comparison of the relative quenching efficiency of the five *n*-NS quenchers can be obtained by comparing the quenching efficiencies at a single value of $\langle Q \rangle$; e.g. $\langle Q \rangle = 200$. The resulting quintuplet of data points ($QE_1 \ldots QE_5$) can be normalized to the lowest value (QE_5) thus:

$$\overline{QE}_i = QE_i/QE_5 \ (i = 1-5).$$

These normalized values can now be plotted against the depth of the quenching moiety (i.e., the doxyl group) in the membrane as depicted in Fig. 7. Such a plot reflects the transverse or depth proximity of the fluorophore to the quenching group and therefore indicates the transverse position of the tryptophan residue in the membrane. For the individual peptides the following results were obtained.

B/H-21$_1$-OMe (theoretical depth 1.5 Å). Protected and protonated peptide esters exhibit similar behavior. Optimum quenching is achieved by 5-NS, which places its paramagnetic doxyl group at a depth of approx. 6.25 Å from the hydrophilic surface of the membrane. The influence of the quenchers decreases as they are placed deeper in the membrane.

B/H-21$_6$-OMe (theoretical depth 9 Å). The tryptophan fluorophore is placed within the steep gradient of the membrane potential. The quenchers 5-, 7-, 10-NS whose doxyl groups are centered at 6.2, 8.7, 12.5 Å, respectively, from the surface show a stronger effect than 12- and 16-NS, which bury the doxyl moiety in the interior of the membrane. Obviously, the fluorophore is shifted somewhat from the theoretical depth towards the surface.

B/H-21$_{11}$-OMe (theoretical depth 16.5 Å). A highly pronounced change in the Stern-Volmer-plot can be observed, and charged and uncharged helices show similar behavior. Optimum quenching is now achieved by deeper quenchers (10-, 12-, 16-NS). Remarkably, 12-NS quenches with high efficiency, although it is a poor quencher in other cases. Thus, the tryptophan fluorophore is assumed to be placed approx. 15 Å from the bilayer surface.

B/H-21$_{16}$-OMe (theoretical depth 24 Å). N-protected and deprotected species behave differently in this case, although the N-terminus of H-21$_{16}$-OMe is bound to the membrane surface by its positive charge, the peptide shows similar accessibility for all quenchers. Optimum quenching efficiency is achieved for 10-NS, corresponding to a depth of 24.5 Å.

In contrast, the fluorophore of B-21$_{16}$-OMe is mostly accessible to the outer quenchers 5- and 7-NS, thus resembling B-21$_6$-OMe. As evaluated from its CD-spectrum, B-21$_{16}$-OMe has an α-helical content of about 50%. Obviously tryptophan at position 16 causes high conformational flexibility, and thus this molecule is unlikely to form a rigid dipole which spans the membrane.

B/H-21$_{21}$-OMe (theoretical depth 31.5 Å). We would expect the tryptophan fluorophore of this peptide to be placed in the hydrophilic section of the membrane, with 5-NS being an optimum quencher. The observed Stern-Volmer plot confirms the expected orientation (Fig. 7).

Other studies on the fluorescence of ionophores in lipid bilayers have been reported. The association of a synthetic N-terminally dansylated nonapeptide of emericin with phosphatidylcholine liposomes has been studied by Nagaraj and Balaram [19], and the behavior of N-dansylated 13- and 17-residue fragments of alamethicin has been examined in liposomes and rat liver mitochondria [20,21]. The self-association of melittin and its binding to lipid vesicles has been investigated by using the fluorescence of the intrinsic tryptophan residue [22,23]. These studies are noteworthy because of some similarities of melittin to alamethicin [4] with respect to α-helical conformation [24,25], lytic properties [26], stimulation of membrane-bound enzymes [27], and high dipole moment [28]. The recent finding of a naturally occurring analog of alamethicin named trichorzianine AIIIc [29] carrying a C-terminal tryptophanol residue is most interesting in the light of our studies on the 21-peptide helices carrying N- and C-terminal tryptophan residues. C-terminally dansylated alamethicin [30] and trichotoxin [4] have been used already in voltage-dependent bilayer experiments, but not in fluorescence spectroscopic studies.

Conclusion

Tryptophan residues at the N- or C-terminal positions in the peptide are situated in a hydro-

philic environment near the bilayer surface. For H-21_1-OMe this is not surprising, as the positive charge is situated on the amino group of tryptophan itself. The experimental behavior of the other synthetic polypeptides proves the original assumption of long helical structures capable of spanning the membrane.

On the other hand, the peptides B/H-21_{11}-OMe would be expected to locate their tryptophan residues in the lipophilic interior of the membrane. This expectation is borne out by experiment.

The compounds B/H-21_6-OMe and H-21_{16}-OMe locate their fluorophores within the steep gradient of the membrne potential. Here small deviations from the theoretical depth of the fluorophores may obscure the differences in quenching efficiency for the *n*-doxyl stearic acids, as shown in the Stern-Volmer-plots for these compounds.

Acknowledgements

This study has been supported by the Deutsche Forschungsgemeinschaft (SFB 76, project B2; G.J.) and by the Australian Research Grants Committee (W.H.S.). K.-P.V. was a stipendiate of the Studienstiftung des Deutschen Volkes.

References

1 Schmitt, H. and Jung, G. (1985) Liebigs Ann. Chem. 321–344
2 Katz, E., Aydin, M., Lucht, N., König, W.A., Ooka, T. and Jung, G. (1985) Liebigs Ann. Chem. 1041–1062
3 Brückner, H., König, W.A., Aydin, M. and Jung, G. (1985) Biochim. Biophys. Acta 827, 51–62
4 Hanke, W., Methfessel, C., Wilmsen, H.-U., Katz, E., Jung, G. and Boheim, G. (1983) Biochim. Biophys. Acta 727, 108–114
5 Jung, G., Katz, E., Schmitt, H., Voges, K.-P. and Boheim, G. (1983) in Physical Chemistry of Transmembrane Ion Motions (Spach, G., ed.), Elsevier, Amsterdam; (1963) Stud. Phys. Theor. Chem. 24, 349–357
6 Menestrina, G., Voges, K.-P., Jung, G. and Boheim, G. (1986) Biophys. J., in the press
7 Boheim, G., Hanke, W. and Jung, G. (1983) Biophys. Struct. Mech. 9, 181–191
8 Jung, G. (1984) in Synthetic Antigens, Proc. Int. Conf. Annali Sclavo 1984, 191–208
9 Blatt, E. and Sawyer, W.H. (1985) Biochim. Biophys. Acta 822, 43–62
10 Blatt, E., Chatelier, R.C. and Sawyer, W.H. (1984) Photochem. Photobiol. 39, 477–483
11 Chatelier, R.C., Blatt, E. and Sawyer, W.H. (1984) Chem. Phys. Lipids 36, 131–136
12 Blatt, E., Chatelier, R.C. and Sawyer, W.H. (1984) Chem. Phys. Lett. 108, 397–400
13 Schmitt, H., Winter, W., Bosch, R. and Jung, G. (1982) Liebigs Ann. Chem., 1304–1321
14 Voges, K.-P. (1985) Dissertation, University Tübingen
15 Jung, G., Voges, K.-P., Schmitt, H., Becker, G., Kolshorn, H. and Albert, K. (1984) in Forum Peptides (Castro, B. and Martinez, J., eds.), pp. 217–220, Centre de Pharmacologie-Endocrinologie, Montpellier
16 Rizzo, V., Schwarz, G., Voges, K.-P. and Jung, G. (1985) Eur. Biophys. J. 12, 67–73
17 Blatt, E., Chatelier, R.C. and Sawyer, W.H. (1986) Biophys. J. 50, 349–356
18 Chou, P.Y. and Fasman, G.D. (1977) Adv. Enzymol. 47, 45–148
19 Nagaraj, R. and Balaram, P. (1979) Biochem. Biophys. Res. Commun. 89, 1041–1049
20 Mathew, M.K., Nagaraj, R. and Balaram, P. (1979) Biochim. Biophys. Acta 649, 339–342
21 Mathew, M.K. Nagarai, R. and Balaram, P. (1981) J. Biol. Chem. 257, 2170–2176
22 Dufourcq, J. and Faucon, J.-F. (1977) Biochim. Biophys. Acta 467, 1–11
23 Faucon, J.-F., Bufourcq, J. ad Loussan, C. (1979) FEBS Lett. 102, 187–190
24 Fox, R.O. and Richards, F.M. (1981) Nature 300, 325–330
25 Terwilliger, T.C., Weissman, L. and Eisenberg, D. (1982) Biophys. J. 37, 353–361
26 Irmscher, G. and Jung, G. (1976) Eur. J. Biochem. 80, 165–174
27 Klumpp, S., Jung, G. and Schultz, J.E. (1984) Biochim. Biophys. Acta 800, 145–151
28 Sano, T. and Schwarz, G. (1983) Biochim. Biophys. Acta 745, 189–193
29 Bodo, B., Rebufrats, S., ElHajji, M. and Davoust, D. (1985) J. Am. Chem. Soc. 107, 6011–6017
30 Eisenberg, M., Kleinberg, M.E. and Shaper, J.H. (1977) Ann. N.Y. Acad. Sci. 303, 291–291